

# Hadroproduction of electroweak gauge boson plus jets and TMD parton density functions

S. Dooling,<sup>1</sup> F. Hautmann,<sup>2,3,4</sup> and H. Jung<sup>1,5</sup>

<sup>1</sup>*Deutsches Elektronen Synchrotron, D-22603 Hamburg*

<sup>2</sup>*Dept. of Physics and Astronomy, University of Sussex, Brighton BN1 9QH*

<sup>3</sup>*Rutherford Appleton Laboratory, Chilton OX11 0QX*

<sup>4</sup>*Dept. of Theoretical Physics, University of Oxford, Oxford OX1 3NP*

<sup>5</sup>*Elementaire Deeltjes Fysica, Universiteit Antwerpen, B 2020 Antwerpen*

## Abstract

If studies of electroweak gauge boson final states at the Large Hadron Collider, for Standard Model physics and beyond, are sensitive to effects of the initial state's transverse momentum distribution, appropriate generalizations of QCD shower evolution are required. We propose a method to do this based on QCD transverse momentum dependent (TMD) factorization at high energy. The method incorporates experimental information from the high-precision deep inelastic scattering (DIS) measurements, and includes experimental and theoretical uncertainties on TMD parton density functions. We illustrate the approach presenting results for production of  $W$ -boson +  $n$  jets at the LHC, including azimuthal correlations and subleading jet distributions.

The associated production of an electroweak gauge boson and hadronic jets is central to many aspects of the Large Hadron Collider (LHC) physics program. It is an important background to Higgs boson and top quark studies, and to supersymmetry and dark matter searches [1]. It provides benchmark observables for studies of QCD, Monte Carlo event generators and parton density functions [2]. In the upcoming high-luminosity runs, it can be used in combination with Higgs boson production [3, 4] for precision studies of QCD initial-state effects beyond fixed-order perturbation theory.

Baseline predictions are obtained from next-to-leading-order (NLO) perturbative matrix elements for the hard, high- $p_\perp$  process, matched with parton showers describing the collinear evolution of the jets developing from the hard event [5]. When this perturbative QCD picture is pushed to higher and higher energies  $\sqrt{s}$ , however, new effects arise in the jet multiplicity distributions and the structure of angular correlations, due to soft but finite-angle multi-gluon emission. As was noted already long ago [6], these high-energy effects can be taken into account by treating the QCD evolution of the initial-state parton distributions via transverse-momentum dependent branching algorithms coupled [7] to hard matrix elements at fixed transverse momentum. This allows one to include soft gluon coherence [8] not only for collinear-ordered emissions but also in the non-ordered region that opens up at high  $\sqrt{s}/p_\perp$  and large  $p_\perp$ . (Examples of angular correlations in multi-jet deep inelastic scattering (DIS) final states are studied in [9]. See e.g. [10] and references therein.)

Besides these dynamical effects, the role of including the correct transverse-momentum kinematics in branching algorithms describing QCD evolution in Monte Carlo event generators has recently been emphasized in [11, 12], and connected with experimental observations of  $p_\perp$  spectra at the LHC [13] in the case of jets produced at moderately non-central rapidities. It has been pointed out [11, 12] that collinear approximations, combined with energy-momentum conservation constraints, give rise to non-negligible kinematic shifts in longitudinal momentum distributions, and are responsible for a large fraction of parton showering corrections to LHC jet final states [13].

In this paper we propose an approach to electroweak boson plus jets production which addresses both the dynamical and kinematical issues mentioned above via transverse-momentum dependent (TMD) QCD evolution equations, and corresponding parton density functions and perturbative matrix elements. Traditional approaches to electroweak boson production taking into account the initial state's transverse momentum distribution have focused on the boson spectrum in the low- $p_\perp$  Sudakov region, and on the treatment of large logarithms for transverse momenta small compared to the boson invariant mass. Our work treats physical effects which persist at high  $p_\perp$  and can affect final states with high jet multiplicities. To this end we use the transverse-momentum dependent QCD factorization [7], which is valid up to arbitrarily large  $p_\perp$ . We couple this with CCFM [8] evolution equations for TMD gluon and valence quark densities using the results recently obtained in [14].

This theoretical framework, although not limited in  $p_\perp$ , is based on the high-energy expansion  $\sqrt{s} \rightarrow \infty$ . Non-asymptotic contributions are included through CCFM matching with soft-gluon terms in the evolution kernels and through subleading effects in the flavor non-singlet sector according to the method of [14]. In [14] this approach is applied to deep inelastic scattering (DIS) and charm quark production and confronted with high-precision combined HERA data [15, 16], which imply small longitudinal momentum fractions  $x$ . In contrast, the subject of this paper explores processes which mostly occur when the values of  $x$  are not very small. It tests the matching procedure and the non-asymptotic contributions. By this calculation, we push the limits of the high-energy expansion beyond the

small- $x$  region, in a manner which can be controlled using the estimation of theoretical and experimental uncertainties on TMD distributions proposed in [14] within the **herafitter** framework [16, 17]. Given the complexity of the final states considered, this is a challenging problem. The results are however encouraging. Moreover, they are sufficiently general to be of interest to any approach that employs TMD formalisms in QCD to go beyond fixed-order perturbation theory and appropriately take account of nonperturbative effects. This will be relevant both to precision studies of Standard Model physics and to new physics searches for which gauge boson plus jets production is an important background.

Using the parton branching Monte Carlo implementation of TMD evolution developed in [14] we make predictions, including uncertainties, for final-state observables associated with  $W$ -boson production. We study jet transverse momentum spectra and azimuthal correlations. In particular, we examine subleading jet distributions, measuring the transverse momentum imbalance between the vector boson and the leading jet.

The starting point of our approach is to apply QCD high-energy factorization [7] at fixed transverse momentum to electroweak gauge boson + jet production,  $q + g^* \rightarrow V + q$ , where  $V$  denotes a gauge boson and  $g^*$  an off-shell gluon. The basic observation is that this factorization allows one to sum high-energy logarithmic corrections for  $\sqrt{s} \rightarrow \infty$  to all orders in the QCD coupling provided the spacelike evolution of the off-shell gluon includes the full BFKL anomalous dimension for longitudinal momentum fraction  $x \rightarrow 0$  [18]. The CCFM evolution equation [8] is an exclusive branching equation which satisfies this property. In addition, it includes finite- $x$  contributions to parton splitting, incorporating soft-gluon coherence for any value of  $x$ . The evolution equation reads [8, 9]

$$\begin{aligned} \mathcal{A}(x, k_t, p) = & \mathcal{A}_0(x, k_t, p) + \int \frac{dz}{z} \int \frac{dq^2}{q^2} \Theta(p - zq) \\ & \times \Delta(p, zq) \mathcal{P}(z, q, k_t) \mathcal{A}\left(\frac{x}{z}, k_t + (1 - z)q, q\right) , \end{aligned} \quad (1)$$

where  $\mathcal{A}(x, k_t, p)$  is the TMD gluon density function, depending on longitudinal momentum fraction  $x$ , transverse momentum  $k_t$  and evolution variable  $p$ . The first term in the right hand side of Eq. (1) is the contribution of the non-resolvable branchings between starting scale  $q_0$  and evolution scale  $p$ , while the integral term in the right hand side of Eq. (1) gives the  $k_t$ -dependent branchings in terms of the Sudakov form factor  $\Delta$  and unintegrated splitting function  $\mathcal{P}$ . Unlike ordinary, integrated splitting functions, the latter encodes soft-virtual contributions into the non-Sudakov form factor [8, 9].

In this framework the vector boson production cross section has the form

$$\sigma^{(V)} = \int \mathcal{A} \otimes H_{qg} \otimes \mathcal{B} , \quad (2)$$

where the symbol  $\otimes$  denotes convolution in both longitudinal and transverse momenta,  $\mathcal{A}$  is the gluon density function obeying Eq. (1),  $H$  is the off-shell (but gauge-invariant) continuation of the  $qg$  hard-scattering function specified by the high-energy factorization [7], and  $\mathcal{B}$  is the valence quark density function introduced at unintegrated level according to the method [19], such that it obeys a modified CCFM branching equation. Explicit calculations for  $H$  are carried out in [20–23] with off-shell partons [24, 25].<sup>1</sup>

<sup>1</sup> Ref. [26] provides an approach to vector boson plus jets also inspired by QCD high-energy factorization [7].

This approach differs from that of the present paper as it is based on matching tree-level  $n$ -parton amplitudes with BFKL amplitudes in the multi-Regge kinematics, treating initial-state partons as collinear. TMD parton density functions and  $k_t$ -dependent branching evolution do not enter in the approach [26].

The  $\mathcal{A}_0$  term in the right hand side of Eq. (1), and the analogous term in the modified CCFM branching equation for the quark distribution  $\mathcal{B}$  [19], depend on nonperturbative parton distributions at scale  $q_0$ , which are to be determined from fits to experimental data. We here use the determination [14] from the precision measurements of the  $F_2$  structure function [16] in the range  $x < 0.005$ ,  $Q^2 > 5 \text{ GeV}^2$ , and the precision measurements of the charm structure function  $F_2^{(\text{charm})}$  [15] in the range  $Q^2 > 2.5 \text{ GeV}^2$ . Good fits to  $F_2$  and  $F_2^{(\text{charm})}$  are obtained (with the best fit to  $F_2^{(\text{charm})}$  giving  $\chi^2$  per degree of freedom  $\chi^2/\text{ndf} \simeq 0.63$ , and the best fit to  $F_2$  giving  $\chi^2/\text{ndf} \simeq 1.18$  [14]). Despite the limited kinematic range, the great precision of the combined data [15, 16] provides a compelling test of the approach at small  $x$ . The production of final states with  $W$  boson and multiple jets at the LHC receives contributions from a non-negligible fraction of events with large separations in rapidity between final-state particles [27], calling for parton branching methods beyond the collinear approximation [6]. On the other hand, the average values of longitudinal momentum fractions  $x$  at which the gluon density is sampled in the  $W$ -boson + jets cross sections at the LHC are not very small. Moreover, quark's average momentum fractions are moderate, and quark density contributions matter [21] at TMD level. For these reasons,  $W$  + jets pushes the limits of the approach probing it in a region where its theoretical uncertainties increase [28], and where the DIS experimental data [15, 16] do not constrain well the TMD gluon distribution.

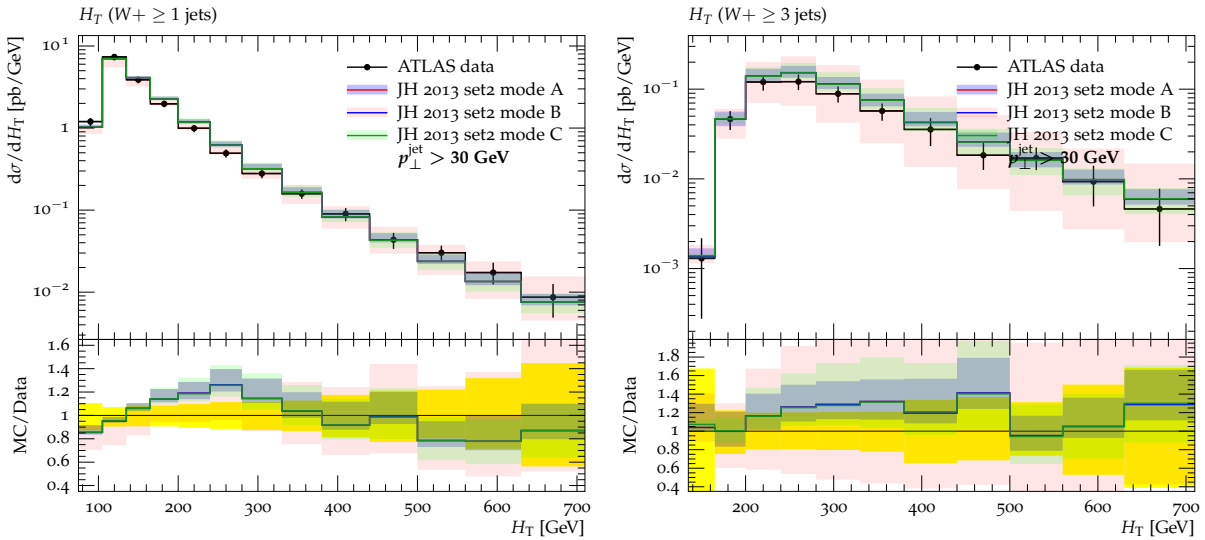


FIG. 1. Total transverse energy  $H_T$  distribution in final states with  $W$ -boson +  $n$  jets at the LHC, for (left)  $n \geq 1$ , (right)  $n \geq 3$ . The purple, pink and green bands correspond to mode A, mode B and mode C as described in the text. The experimental data are from [30], with the experimental uncertainty represented by the yellow band.

The numerical results that follow are obtained using the RIVET - package [29]. We use the TMD distribution set JH-2013-set2 [14]. We compare the results with the ATLAS measurements [30] (jet rapidity  $|\eta| < 4.4$ ) and CMS measurements [31] (jet rapidity  $|\eta| < 2.4$ ). The uncertainties on the predictions are determined according to the method [14]. This treats experimental and theoretical uncertainties. Experimental pdf uncertainties are obtained within the `herafitter` package following the procedure of [32]. Theoretical uncertainties are considered separately due to the variation of the starting scale  $q_0$  for evolution, the

renormalization scale  $\mu_r$  for the strong coupling, the factorization scale  $\mu_f$ . We apply this method in different modes: mode A (purple band in the plots) includes uncertainties due to the renormalization scale, starting evolution scale, and experimental errors; mode B (pink band in the plots) and mode C (green band in the plots) also include factorization scale uncertainties. These are estimated as follows.

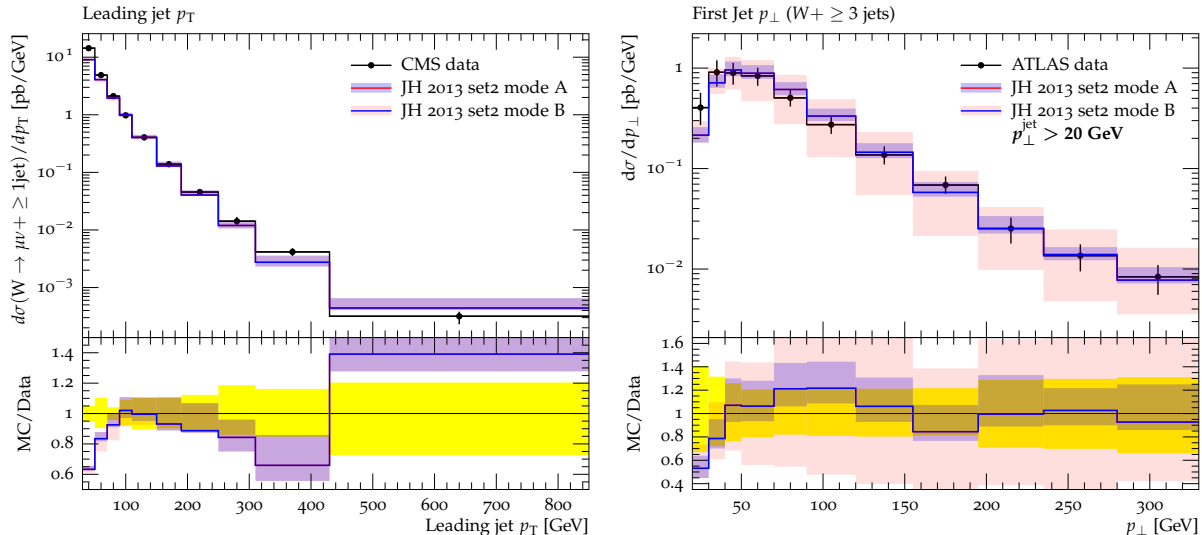


FIG. 2. Leading jet  $p_T$  spectra in  $W$ -boson +  $n$  jets: (left) inclusive; (right)  $n \geq 3$ . The purple and pink bands correspond to mode A and mode B as described in the text. The experimental data are from [31] (left) and [30] (right), with the experimental uncertainty represented by the yellow band.

We take the central value for the factorization scale to be  $\mu_f^2 = m^2 + q_\perp^2$ , where  $m$  and  $q_\perp$  are the invariant mass and transverse momentum of the boson + jet system. The choice of this scale is suggested by the CCFM angular ordering [6, 8, 9] and the maximum angle available to the branching. We then consider two different types of variation of  $\mu_f$ . In mode C, we vary the transverse part of  $\mu_f^2$  by a factor of 2 above and below the central value. In mode B, we decompose  $\mu_f$  as  $\mu_f^2 = m_V^2 + \nu^2$ , where  $m_V$  is the vector boson mass, and vary the dynamical part  $\nu^2$  of  $\mu_f^2$ , again by a factor of 2 above and below the central value. We note that the above variation affects the kinematics of the hard scatter, and the amount of energy available for the shower. While the mode C variation is more closely related to the estimation of unknown higher-order corrections in standard calculations performed under collinear-ordering approximations, the mode B variation is a (conservative) way to estimate uncertainties from possibly enhanced higher orders due to longitudinal momentum kinematics (not considered under standard approximations). For this reason we expect large mode-B uncertainties especially in the case of high multiplicity. One of the limitations of the current treatment is that this variation is applied to the shower but not to the hard matrix element. In a more complete calculation, subject for future investigations, the scale dependence is taken into account in the hard factor, and the pdf fitted to data is also changed [14], unlike the ordinary case of collinear calculations. The net result of these two effects is expected to reduce the uncertainty band. The present treatment, on the other hand, combined with the sensitivity of the process to the medium to large  $x$  region, leads to significant theoretical uncertainties, in particular larger than the experimental uncertainties. Thus, we regard the mode B bands presented in the following as the most conservative

estimate of the uncertainties. We expect mode C bands to be smaller, and intermediate between mode A and mode B. We note that the factorization scale variation plays a different role here than in ordinary collinear calculations.

Fig. 1 shows the total transverse energy distribution  $H_T$  for production of  $W$ -boson +  $n$  jets, for different values of the number of jets  $n$ . We take the minimum jet transverse momentum to be 30 GeV. The main features of the final states are described by the predictions including the case of higher jet multiplicities. The theoretical uncertainties are larger for larger  $H_T$ , corresponding to increasing  $x$ . At fixed  $H_T$ , they are larger for higher jet multiplicities, corresponding to higher probability for jets to be formed from the partonic showers. The comparison of the bands for the three modes described above illustrates that mode C is intermediate between mode A and mode B.

We next consider the spectra of the individual jets. Fig. 2 shows the spectrum of the leading jet associated with the  $W$ -boson, inclusively (left) and for  $n \geq 3$  jets (right). For the sake of simplicity we only show uncertainty bands corresponding to the two extreme cases, A and B (mode C is intermediate between these, similarly to the case of Fig. 1). The CMS [31] (left) and ATLAS [30] (right) measurements cover different ranges in jet rapidity, respectively  $|\eta| < 2.4$  [31] and  $|\eta| < 4.4$  [30]. The plot on the left includes higher values of  $p_\perp$ . Given the computational limitations at finite  $x$  outlined above, the theory comparison with the measurements in Fig. 2 is satisfactory over a broad  $p_\perp$  range. It is noted in [27] that, in

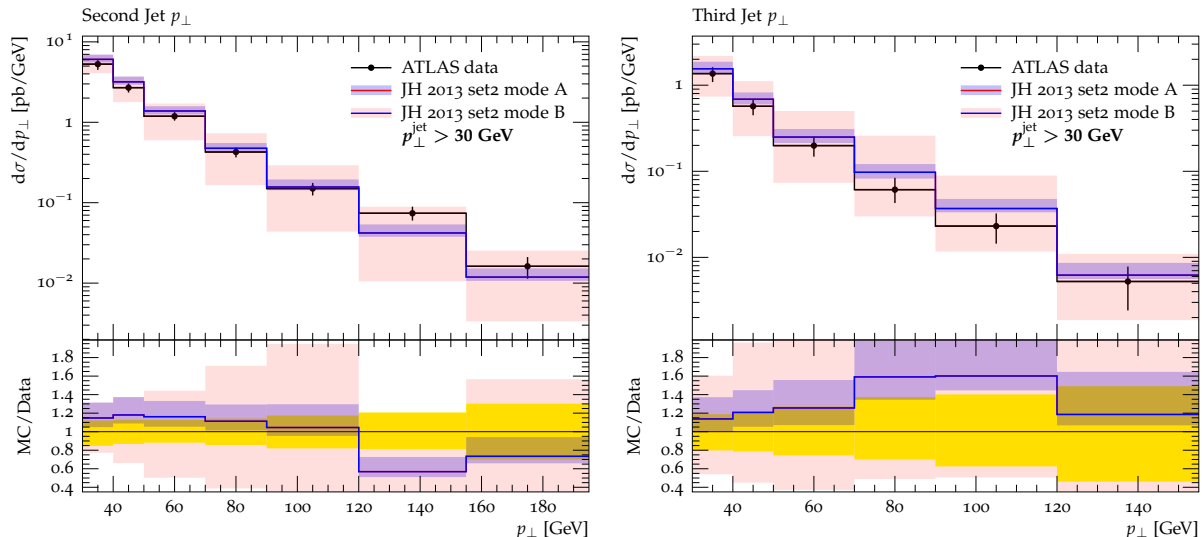


FIG. 3. *Second jet (left) and third jet (right) distributions associated with  $W$ -bosons. The purple and pink bands correspond to mode A and mode B as described in the text. The experimental data are from [30], with the experimental uncertainty represented by the yellow band.*

contrast, the leading-order PYTHIA [33] result strongly deviates from these measurements in the high-multiplicity and the high- $p_\perp$  regions. In such a framework the description of the high- $p_\perp$  region is to be improved by supplementing the parton shower with next-to-leading-order corrections to the matrix element, e.g. via matched NLO-shower calculations [34] such as POWHEG. The TMD formulation with exclusive evolution equations, on the other hand, incorporating at the outset large-angle, finite- $k_\perp$  emissions [9, 35], can describe the shape of the spectra also at large multiplicity and large transverse momentum. We note in particular that the different ranges in rapidity quoted above for the samples [30, 31] play a

non-negligible role, given that our exclusive formalism is designed to treat gluon radiation over large rapidity intervals.

In Fig. 3 we look into the multi-jet final states in closer detail by examining the  $p_\perp$  spectra of the second jet and the third jet associated with  $W$  production. We see that not only the leading jet and global distributions of Figs. 2 and 1 but also the detailed shapes of the subleading jets in Fig. 3 can be obtained from the TMD formalism. The uncertainty bands, on the other hand, increase as we go to higher jet multiplicity. The effect is moderate for mode A, but pronounced for the conservative mode B.

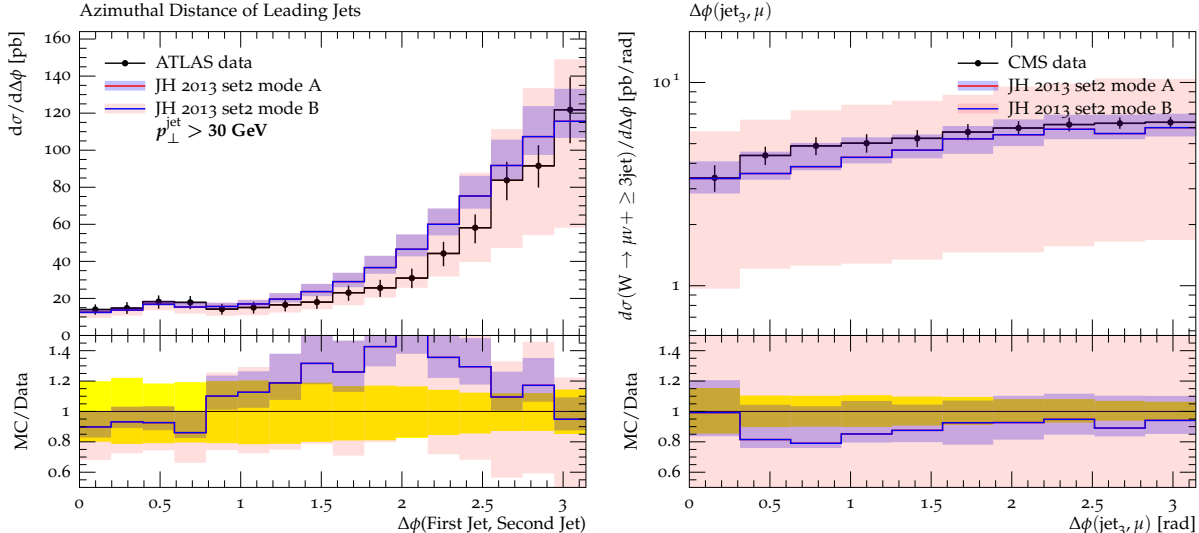


FIG. 4. (left) Azimuthal distance of the leading jets associated with  $W$ -bosons; (right) azimuthal correlation of the third jet to the  $W$ . The purple and pink bands correspond to mode A and mode B as described in the text. The experimental data are from [30] (left) and [31] (right), with the experimental uncertainty represented by the yellow band.

In Fig. 4 we turn to angular correlations. We consider two examples: the distribution in the azimuthal separation  $\Delta\phi$  between the two hardest jets (left); the correlation of the third jet to the  $W$ -boson (right). As noted earlier, predictions of the structure of angular correlations are a distinctive feature of the TMD exclusive formulation. The shape of the experimental measurements is well described, within the theoretical uncertainties, both at large  $\Delta\phi$  and down to the decorrelated, small- $\Delta\phi$  region.

In conclusion, this work shows how exclusive evolution equations in QCD at high energies can be used to take into account QCD contributions to the production of electroweak bosons plus multi-jets due to finite-angle soft gluon radiation, and estimate the associated theoretical uncertainties. This will be relevant both to precision studies of Standard Model physics and to new physics searches for which vector boson plus jets are an important background.

Unlike traditional approaches to electroweak boson production including effects of the initial state's transverse momentum in the low- $p_\perp$  region, the formulation of TMD pdfs and factorization employed in this work incorporates physical effects which persist at high  $p_\perp$  and treats final states of high multiplicity. The effects studied come from multiple gluon emission at finite angle and the associated color coherence [6, 8, 9], and are present to all orders in the strong coupling  $\alpha_s$ . In particular, they are beyond next-to-leading-order perturbation theory matched with collinear parton showers [5]. They can contribute significantly to the

estimate of theoretical uncertainties in multi-jet distributions at high energies.

The method of this work incorporates the experimental information from the high-precision DIS combined measurements [15, 16]. The use of the TMD density determined [14] from these measurements in the comparison with the LHC  $W + n$ -jet data indicates that detailed features of the associated final states can be obtained both for the leading jet and the subleading jets. It underlines the consistency of the physical picture which can be extended from DIS to Drell-Yan processes to describe QCD multi-jet dynamics. It also points to the relevance of Monte Carlo event generators which aim at including parton branching at transverse momentum dependent level (see e.g. [36, 37]).

Future applications may employ vector boson  $pp$  data to advance our knowledge of transverse momentum parton distributions [17, 38]. Vector boson plus jets are a benchmark process for QCD studies of multi-parton interactions [39], and may help shed light on topical issues in the physics of forward jet production [40]. A program combining Drell-Yan and Higgs measurements can become viable at high luminosity [3] to carry out precision QCD studies accessing gluon transverse momentum and polarization distributions [3, 4].

## ACKNOWLEDGMENTS

We thank D. Baumgartel for help with the CMS preliminary RIVET plug-in.

- 
- [1] O. Buchmueller, talk at EPS HEP 2013 Conference, July 2013; C. Issever, talk at SUSY 2013, ICTP, August 2013.
  - [2] S. Alekhin *et al.*, arXiv:1101.0536 [hep-ph].
  - [3] P. Ciproiano *et al.*, Phys. Rev. D **88** (2013) 097501; F. Hautmann, Phys. Lett. B **535** (2002) 159.
  - [4] D. Boer, W.J. den Dunnen, C. Pisano, M. Schlegel and W. Vogelsang, Phys. Rev. Lett. **108** (2012) 032002.
  - [5] S. Höche, F. Krauss, M. Schönherr and F. Siegert, Phys. Rev. Lett. **110** (2013) 052001.
  - [6] G. Marchesini and B.R. Webber, Nucl. Phys. **B386** (1992) 215, Nucl. Phys. **B349** (1991) 617.
  - [7] S. Catani, M. Ciafaloni and F. Hautmann, Phys. Lett. B **242** (1990) 97; Nucl. Phys. **B366** (1991) 135; Phys. Lett. **B307** (1993) 147; S. Catani and F. Hautmann, Phys. Lett. **B315** (1993) 157; Nucl. Phys. **B427** (1994) 475.
  - [8] M. Ciafaloni, Nucl. Phys. **B296** (1988) 49, S. Catani, F. Fiorani and G. Marchesini, Nucl. Phys. **B336** (1990) 18, G. Marchesini, Nucl. Phys. **B445** (1995) 49.
  - [9] F. Hautmann and H. Jung, JHEP **0810** (2008) 113; arXiv:0712.0568; arXiv:0804.1746.
  - [10] F. Hautmann, arXiv:0909.1240 [hep-ph].
  - [11] S. Dooling *et al.*, Phys. Rev. D **87** (2013) 094009; arXiv:1304.7180 [hep-ph]; PoS DIS2013 (2013) 156.
  - [12] F. Hautmann and H. Jung, Eur. Phys. J. C **72** (2012) 2254; Nucl. Phys. Proc. Suppl. **234** (2013) 51; F. Hautmann, arXiv:1304.8133 [hep-ph].
  - [13] ATLAS Coll. (G. Aad *et al.*), Phys. Rev. D **86** (2012) 014022; CMS Coll. (S. Chatrchyan *et al.*), Phys. Rev. D **87** (2013) 112002; Phys. Rev. Lett. **107** (2011) 132001.
  - [14] F. Hautmann and H. Jung, Nucl. Phys. **B883** (2014) 1.



- [15] H. Abramowicz *et al.*, Eur. Phys. J. C **73** (2013) 2311.
- [16] F. Aaron *et al.*, JHEP **1001** (2010) 109.
- [17] “HERAFitter” (2012), <https://www.herafitter.org/>; F. Aaron *et al.*, Eur. Phys. J. **C64** (2009) 561; F. James and M. Roos, Comput. Phys. Commun. **10** (1975) 343.
- [18] L.N. Lipatov, Phys. Rept. **286** (1997) 131; V. S. Fadin, E. A. Kuraev and L. N. Lipatov, Phys. Lett. B **60** (1975) 50; I. I. Balitsky and L. N. Lipatov, Sov. J. Nucl. Phys. **28** (1978) 822.
- [19] M. Deak, F. Hautmann, H. Jung and K. Kutak, arXiv:1012.6037 [hep-ph]; Eur. Phys. J. C **72** (2012) 1982; arXiv:1206.7090 [hep-ph]; PoS ICHEP2010 (2010) 108.
- [20] R.D. Ball and S. Marzani, Nucl. Phys. B **814** (2009) 246; arXiv:0906.4729 [hep-ph].
- [21] F. Hautmann, M. Hentschinski and H. Jung, Nucl. Phys. B **865** (2012) 54; arXiv:1205.6358 [hep-ph]; arXiv:1207.6420 [hep-ph]; arXiv:1209.6305 [hep-ph].
- [22] A. van Hameren, P. Kotko and K. Kutak, JHEP **1301** (2013) 078; A. van Hameren, K. Kutak and T. Salwa, Phys. Lett. B **727** (2013) 226.
- [23] S.P. Baranov, A.V. Lipatov and N.P. Zotov, Phys. Rev. D **89** (2014) 094025.
- [24] A.V. Bogdan and V.S. Fadin, Nucl. Phys. B **740** (2006) 36.
- [25] L.N. Lipatov and M.I. Vyazovsky, Nucl. Phys. B **597** (2001) 399.
- [26] J.R. Andersen, T. Hapola and J.M. Smillie, JHEP **1209** (2012) 047.
- [27] F. Hautmann and H. Jung, PoS DIS2013 (2013) 157; PoS Photon2013 (2014) 003.
- [28] F. Hautmann and H. Jung, PoS DIS2013 (2013) 053; arXiv:1206.1796 [hep-ph].
- [29] A. Buckley, J. Butterworth, L. Lönnblad, D. Grellscheid, H. Hoeth *et al.*, Rivet user manual, Comput. Phys. Commun. **184** (2013) 2803.
- [30] G. Aad *et al.* (ATLAS Coll.), Phys. Rev. D **85** (2012) 092002.
- [31] V. Khachatryan *et al.* (CMS Coll.), arXiv:1406.7533 [hep-ex].
- [32] J. Pumplin, D. Stump, R. Brock, D. Casey, J. Huston, J. Kalk, H.-L. Lai and W.-K. Tung, Phys. Rev. **D65** (2001) 014013; Phys. Rev. **D65** (2001) 014012.
- [33] T. Sjöstrand, S. Mrenna and P. Skands, Comput. Phys. Commun. **178** (2008) 852.
- [34] P. Nason and B.R. Webber, Ann. Rev. Nucl. Part. Sci. **62** (2012) 187.
- [35] F. Hautmann, Acta Phys. Polon. B **40** (2009) 2139; PoS ICHEP2010 (2010) 150; Phys. Lett. B **655** (2007) 26.
- [36] S. Jadach, M. Jezabek, A. Kusina, W. Placzek and M. Skrzypek, Acta Phys. Polon. B **43** (2012) 2067.
- [37] H. Jung *et al.*, Eur. Phys. J. C **70** (2010) 1237.
- [38] S. Mert Aybat and T.C. Rogers, Phys. Rev. D **83** (2011) 114042.
- [39] G. Aad *et al.* (ATLAS Coll.), New. J. Phys. **15** (2013) 033038.
- [40] F. Hautmann, Acta Phys. Polon. B **44** (2013) 761; arXiv:1205.5411 [hep-ph]; M. Grothe *et al.*, arXiv:1103.6008 [hep-ph]; M. Deak *et al.*, JHEP **0909** (2009) 121.